Charge Fluctuations in Nanoscale Capacitors

David T. Limmer,[1] Céline Merlet,[2,3] Mathieu Salanne,[2,3] David Chandler,[1] Paul A. Madden,[4] René van Roij,[5] and Benjamin Rotenberg[2,3,*]

[1]*Department of Chemistry, University of California, Berkeley, California 94720, USA*
[2]*UPMC Univ-Paris 06 and CNRS, UMR 7195, PECSA, F-75005, Paris, France*
[3]*Réseau sur le Stockage Electrochimique de l'Energie (RS2E), FR CNRS 3459, France*
[4]*Department of Materials, University of Oxford, Parks Road, Oxford OX1 3PH, United Kingdom*
[5]*Institute for Theoretical Physics, Utrecht University, 3584 CE Utrecht, The Netherlands*

(Received 28 June 2013; published 4 September 2013)

The fluctuations of the charge on an electrode contain information on the microscopic correlations within the adjacent fluid and their effect on the electronic properties of the interface. We investigate these fluctuations using molecular dynamics simulations in a constant-potential ensemble with histogram reweighting techniques. This approach offers, in particular, an efficient, accurate, and physically insightful route to the differential capacitance that is broadly applicable. We demonstrate these methods with three different capacitors: pure water between platinum electrodes and a pure as well as a solvent-based organic electrolyte each between graphite electrodes. The total charge distributions with the pure solvent and solvent-based electrolytes are remarkably Gaussian, while in the pure ionic liquid the total charge distribution displays distinct non-Gaussian features, suggesting significant potential-driven changes in the organization of the interfacial fluid.

DOI: 10.1103/PhysRevLett.111.106102 PACS numbers: 68.08.−p, 05.40.−a, 82.47.Uv

The charge of an electrode in contact with a liquid and maintained at a constant potential undergoes thermal fluctuations that encode information on microscopic interfacial processes. Most common applications involving such interfaces, such as charge storage in dielectric or electrochemical double layer capacitors [1], electrochemistry, water purification, or the growing field of ''blue energy'' [2–4], utilize only the ability of the metal to acquire an average charge upon application of voltage. However, it is also possible to extract microscopic information on the interfacial processes from the fluctuation of the electrode charge, both near and far from equilibrium, from the large-deviation statistics of fluctuations of the electrode charge. Our purpose here is to demonstrate this fact and to add to the tools available to exploit it.

As nanoscale devices become widely available, it is essential to better understand these fluctuations. Experimentally, this possibility is rarely exploited, with the notable exceptions of electrochemical noise analysis to infer redox reaction rates and information on corrosion processes [5,6] or more recently electrochemical correlation spectroscopy for single molecule detection and ultralow flow rate measurements in nanofluidic channels [7,8]. The opportunities offered by such approaches remain, however, limited by the theoretical tools to interpret the signal and uncover the underlying processes.

Traditional mean-field treatments [9–13], including some models of electric current fluctuations [14,15], ignore the fluctuations we consider. During the past decade, however, molecular simulations have been successfully applied to the study of various metallic electrodes (aluminum, platinum, graphite, nanoporous carbon) and electrolytes (aqueous and organic solutions, molten salts, ionic liquids) [16–21]. In such simulations, it is essential to account for the polarization of the electrode by the ions. In turn, this polarization screens the (effective) interactions between the ions and thereby directly affects the structure and dynamics of the interface [22]. Analytical models accounting for the image charge induced on the electrode [23] remain limited to regular geometries. Nevertheless, efficient algorithms have been introduced to simulate electrodes in which the potential is maintained at a constant value [16,24,25]. The charge on each electrode atom then fluctuates in response to the thermal motion of the fluid and these fluctuations at any instant are significantly heterogeneous. See Fig. 1.

Let $\mathcal{H} = K(\mathbf{p}^N) + U(\mathbf{r}^N, \mathbf{q})$ be the microscopic Hamiltonian of the system with ion positions $\mathbf{r}^N = \{\mathbf{r}_I\}_{I=1,\ldots,N}$, ion momenta $\mathbf{p}^N = \{\mathbf{p}_I\}_{I=1,\ldots,N}$, and electrode charge distribution $\mathbf{q} = \{q_i\}_{i=1,\ldots,2M}$, with $2M$ including the atoms of both electrodes. The electrode atoms are fixed in space. The kinetic part K depends only on the ion momenta, and its contribution to partition functions can be trivially integrated out. Thus, in the following we focus only on the potential part U. The constant-potential ensemble is defined in terms of the potential of each electrode atom $\boldsymbol{\Psi}^0 = \{\Psi_i^0\}_{i=1,\ldots,2M}$. In this ensemble, the charge distribution $\mathbf{q}$ in the electrodes fluctuates as a result of charge exchange with a reservoir, namely, the external circuit which connects the two electrodes. Charging the capacitor from $\mathbf{q} = 0$ to a charge distribution $\mathbf{q}$ under fixed $\boldsymbol{\Psi}^0$ corresponds to a work exchange $\mathbf{q} \cdot \boldsymbol{\Psi}^0$ with this reservoir. Thus, the probability of a state with ion positions $\mathbf{r}^N$ is

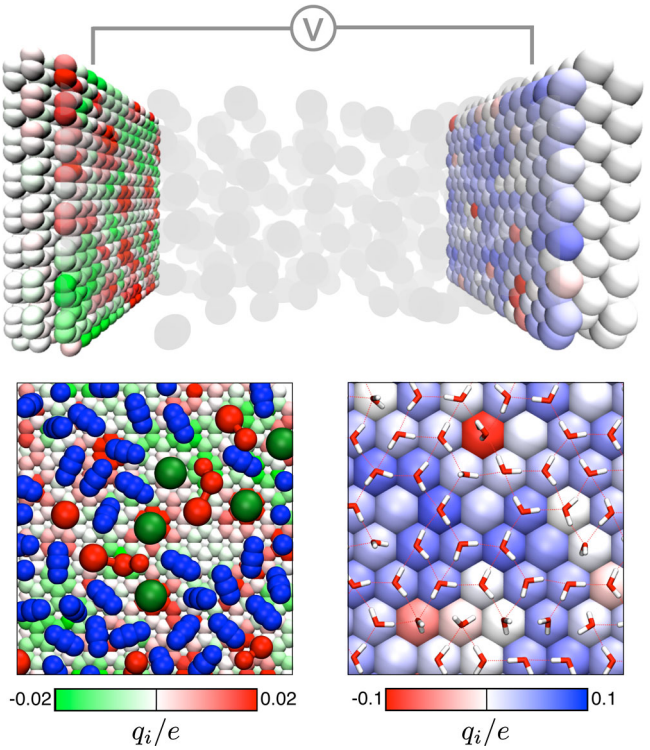

FIG. 1 (color online). Each capacitor consists of an electrolyte between two electrodes maintained at a constant potential difference. The color code on the electrode atoms indicates the instantaneous charge q_i, with the corresponding scale shown at the bottom (darker colors correspond to larger partial charges). The left-hand panels show a graphite electrode, and at the bottom left is a representative configuration of the first adlayer of the 1.5M 1-butyl-3-methylimidazolium (red) hexafluorophosphate (green) in acetonitrile (blue) solution in contact with it. The right-hand panels show the 111 crystal facet of a platinum electrode, and at the bottom right is a representative configuration of the first adlayer of the water in contact with it.

$$P(\mathbf{r}^N|\boldsymbol{\Psi}^0) = \frac{\int d\mathbf{q} e^{-\beta U(\mathbf{r}^N,\mathbf{q})+\beta\mathbf{q}\cdot\boldsymbol{\Psi}^0}}{\int d\mathbf{r}^N d\mathbf{q} e^{-\beta U(\mathbf{r}^N,\mathbf{q})+\beta\mathbf{q}\cdot\boldsymbol{\Psi}^0}}, \quad (1)$$

where $\beta = 1/k_B T$, with k_B Boltzmann's constant and T the temperature.

The integrals can be computed using a saddle point expansion around the charge distribution $\mathbf{q}^*$ minimizing the term in the exponential, which satisfies

$$\left.\frac{\partial U(\mathbf{r}^N,\mathbf{q})}{\partial \mathbf{q}}\right|_{\mathbf{q}=\mathbf{q}^*} = \boldsymbol{\Psi}^0, \quad (2)$$

i.e., such that the potential on each atom is the imposed one. The probability of a state with ion positions $\mathbf{r}^N$ (and corresponding charge distribution $\mathbf{q}^*$) can be expressed exactly using the Legendre transform $\mathcal{U}(\mathbf{r}^N,\boldsymbol{\Psi}^0) = U(\mathbf{r}^N,\mathbf{q}^*) - \mathbf{q}^*\cdot\boldsymbol{\Psi}^0$ as $P(\mathbf{r}^N|\boldsymbol{\Psi}^0) = e^{-\beta\mathcal{U}(\mathbf{r}^N,\boldsymbol{\Psi}^0)}/\mathcal{Z}(\boldsymbol{\Psi}^0)$, with $\mathcal{Z}(\boldsymbol{\Psi}^0) = \int d\mathbf{r}^N e^{-\beta\mathcal{U}(\mathbf{r}^N,\boldsymbol{\Psi}^0)}$.

In practice one is only interested in the case where the potential can take only two values, namely, $\Psi_i^0 = \Psi_+^0$ for all atoms in the positive electrode and $\Psi_i^0 = \Psi_-^0$ for all atoms in the negative electrode. This corresponds to the condition of a constant potential inside a metal (perfect conductor). In that case the additional energy term simplifies to $\mathbf{q}^*\cdot\boldsymbol{\Psi}^0 = \sum_{i\in\pm} q_i^*\Psi_i^0 = Q\Delta\Psi$, with $Q = Q^+ = -Q^-$ the total charge of the positive electrode and $\Delta\Psi = \Psi_+^0 - \Psi_-^0$ the potential difference between the electrodes. Note that the sign convention to label the electrodes does not matter. Moreover, the probability of a state, hence any observable property, depends only on $\Delta\Psi$ and not on the absolute value of the potentials, which are defined with respect to a reference electrode not present in the system and which provides charge to the electrodes. Using the above result, we finally rewrite the probability as

$$P(\mathbf{r}^N|\Delta\Psi) = \frac{e^{-\beta U(\mathbf{r}^N,\mathbf{q}^*)+\beta Q\Delta\Psi}}{\mathcal{Z}(\Delta\Psi)}, \quad (3)$$

with the partition function

$$\mathcal{Z}(\Delta\Psi) = e^{-\beta\mathcal{F}(\Delta\Psi)} = \int d\mathbf{r}^N e^{-\beta U(\mathbf{r}^N,\mathbf{q}^*)+\beta Q\Delta\Psi}, \quad (4)$$

and $\mathcal{F}$ the associated free energy. In this ensemble, the average value of any observable $A(\mathbf{r}^N,\mathbf{q}^*)$ is computed as

$$\langle A\rangle = \int d\mathbf{r}^N P(\mathbf{r}^N|\Delta\Psi) A(\mathbf{r}^N,\mathbf{q}^*), \quad (5)$$

where one should keep in mind that the charge distribution $\mathbf{q}^*$ is not a free variable, as it is determined for each ion configuration $\mathbf{r}^N$ by Eq. (2). The average total charge determines the integral capacitance $\mathrm{C_{int}} = \langle Q\rangle/\Delta\Psi$, whereas the differential capacitance is related to the variance of the total charge distribution:

$$\mathrm{C_{diff}} = \frac{\partial\langle Q\rangle}{\partial\Delta\Psi} = \beta\langle\delta Q^2\rangle, \quad (6)$$

with $\delta Q = Q - \langle Q\rangle$. This fluctuation-dissipation relation, which can be derived by considering the derivatives of $\mathcal{Z}$ with respect to $\Delta\Psi$ [26], is known in electronics as the Johnson-Nyquist relation [27,28]. We can also show that the capacitance is related to the charge-charge structure factor inside the electrode [26]:

$$\lim_{k\to 0} S_{qq}(k) = \frac{\mathrm{C_{diff}} k_B T}{M\langle\delta q^2\rangle}, \quad (7)$$

with $\langle\delta q^2\rangle = \langle q^2\rangle - \langle q\rangle^2$ the variance of the distribution of the charge per atom. This result holds for both electrodes, even though $S_{qq}(k)$ may differ for nonzero wave vectors.

The algorithm we use to simulate a metallic electrode maintained at a constant potential follows from the work of Siepmann and Sprik [24], later adapted by Reed *et al.* to the case of electrochemical cells [16]. The electrode consists of explicit atoms bearing a Gaussian charge distribution $\rho_i(\mathbf{r}) = q_i^*\eta^3\pi^{3/2}\exp(-|\mathbf{r}-\mathbf{r}_i|^2\eta^2)$, where η^{-1} is the width of the distribution and where the atomic charge q_i^* of each atom is determined at each time step of the simulation

by minimizing $U_c - \sum_{i\in\pm} q_i \Psi_i^0$, with U_c the Coulomb energy, with respect to all the variable charges simultaneously. Forces acting on the ions are then computed using the minimizing charges.

The distribution of the total charge Q in the constant-potential ensemble is

$$P(Q|\Delta\Psi) = \int d\mathbf{r}^N P(\mathbf{r}^N|\Delta\Psi)\delta\Big(Q - \sum_{i\in+} q_i\Big), \quad (8)$$

with δ the Dirac distribution. The distributions of the total charge can be sampled directly from simulations at the corresponding potentials. However, this sampling is limited to values of the total charge that are close to the average $\langle Q\rangle$. A more accurate estimate can be obtained by combining the data from the simulations performed for various potential differences using histogram reweighting. Indeed, one can show that

$$-\ln P(Q|0) = -\ln P(Q|\Delta\Psi) + \beta Q\Delta\Psi + \beta\Delta\mathcal{F}, \quad (9)$$

with $\Delta\mathcal{F} = \mathcal{F}(\Delta\Psi) - \mathcal{F}(0)$ the difference in free energy [defined by Eq. (4)]. Each simulation under an applied potential thus provides an estimate of the charge distribution at any other potential, up to the unknown constants $\mathcal{F}(\Delta\Psi)$, which are determined self-consistently in the weighted histogram analysis method [29–31]. Such an approach is well established in other contexts, but has not yet been considered for simulations in the constant-potential ensemble.

We investigate several capacitors illustrated in Fig. 1: pure water between platinum electrodes and an organic electrolyte, 1-butyl-3-methylimidazolium hexafluorophosphate (BMI-PF_6), either as a pure ionic liquid or as a 1.5M solution in acetonitrile (MeCN), between graphite electrodes. Details on the systems and molecular models can be found in the Supplemental Material [26]. These combinations of electrodes and electrolytes offer a large contrast of properties: The former is a dielectric capacitor containing only neutral molecules, while the latter contain ions in the gap and are hence "double-layer" capacitors. In addition, in the former case the water molecules form hydrogen bonds and have a size comparable to that of the electrode atoms, while in the latter all ions and molecules are large so that the electrode appears rather smooth on their scale. Figure 1 also shows the local charge distribution on one of the electrodes for instantaneous configurations of the solvent-based systems under a potential difference. It is strikingly heterogeneous and strongly correlated with the local structure of the adsorbed fluid.

Figure 2 shows that fluctuations of the total charge on the electrodes for both solvent-based systems are Gaussian to a remarkable degree. These statistics imply the validity of the linear response theory over the range of charges shown in Fig. 2. The inset shows that $\langle Q\rangle$ is indeed proportional to the applied potential $\Delta\Psi$ with a slope $\beta\langle\delta Q^2\rangle$. Such a comparison not only provides information on the

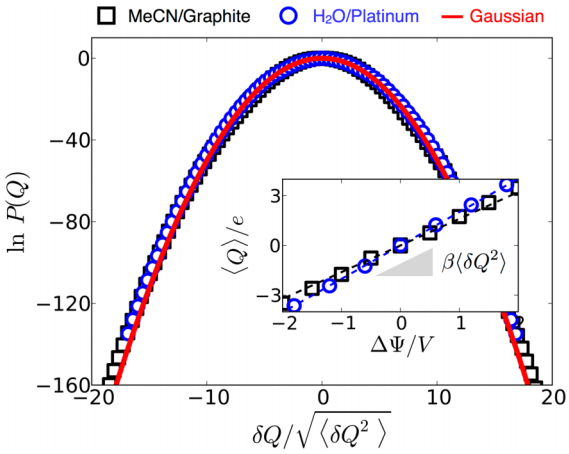

FIG. 2 (color online). Probability distribution of the total charge Q on the electrodes at $\Delta\Psi = 0$ V for the acetonitrile (MeCN) electrolyte and water-based capacitors. The data are reported as a function of $\delta Q/\sqrt{\langle\delta Q^2\rangle}$. The red line is a Gaussian distribution with the same mean and variance. The inset compares the average charge as a function of voltage from simulations (symbols) with lines of slope $\beta\langle\delta Q^2\rangle$. This illustrates the linear response of both systems and the validity of the fluctuation-dissipation relation Eq. (6).

physical properties of these two capacitors, but also demonstrates the relevance of this new approach to determine the differential capacitance. The latter is $\approx 40\%$ larger in the water/Pt case (3.2 versus 2.3 and 2.1 $\mu\mathrm{F}\cdot\mathrm{cm}^{-2}$ for the graphite capacitors with the solution in MeCN and pure ionic liquid, respectively). Continuum theory for water between electrodes in the simulated geometry (distance $d = 5.2$ nm between the surfaces), using the permittivity of the SPC/E water model, predicts a capacitance $\epsilon_0\epsilon_r/d = 11.4\ \mu\mathrm{F}\cdot\mathrm{cm}^{-2}$, indicating that the molecular nature of the interface, which suppresses dipole fluctuations on the surface [32], plays an important role in the overall capacitance (the effective permittivity in the bulk region agrees well with that of SPC/E [17]).

The Gaussian behavior suggests that the charging process for both systems arises from microscopic events that are correlated over only small length scales, those comparable to sizes of molecules. The local charge induced on the electrode by an interfacial molecule or ion can be analyzed in terms of the distribution of individual charges of the electrode atoms. These distributions are reported for both systems as a function of potential in Fig. 3. The bimodal distribution in the case of water at Pt arises from the two possible orientations of OH bonds with respect to the surface, which are asymmetric between the positive and negative electrodes and evolve with the potential, as the macroscopic electric field favors or hinders the formation of a hydrogen bond with the surface [17]. For the organic electrolyte on graphite the behavior is not bimodal, but the distributions are not Gaussian either, where the non-Gaussianity stems from the shape and size asymmetry of

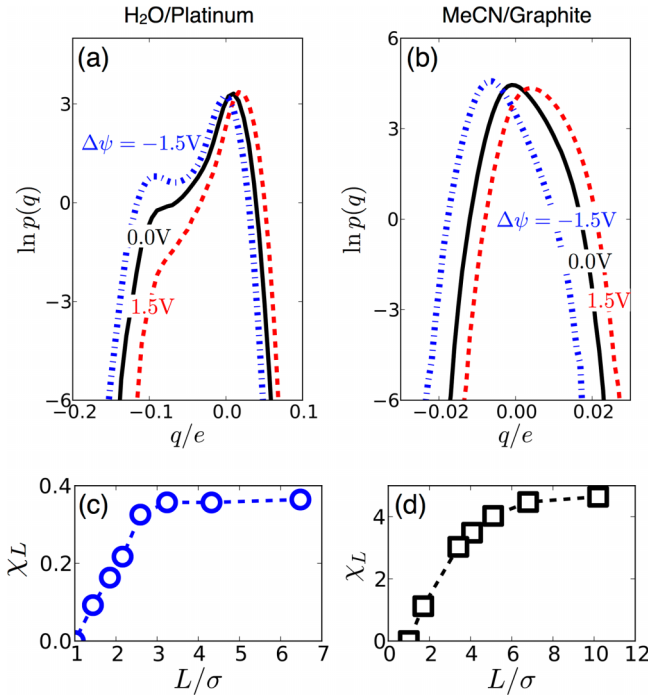

FIG. 3 (color online). Distribution of the charge q_i on electrode atoms for the H_2O/platinum (a) and MeCN-based organic electrolyte/graphite (b) capacitors, inside the electrodes in the absence and presence of voltage ($\Delta\Psi = \pm 1.5$ V refer to the positive and negative electrodes for 1.5 V). (c), (d) Variation of the charge fluctuations χ_L, with increasing electrode area in units of the electrode atom diameter σ (see text).

the ions as well as from the dipolar charge distribution of the acetonitrile molecule. As expected, the larger local charges are induced by nearby ions rather than solvent molecules. As the potential changes, the main change in the distribution is a shift of its mean, rather than its shape, as a result of the gradual change in local composition of the interfacial fluid.

The crossover from the non-Gaussian behavior of the local charge to the Gaussian distribution of Q suggests the existence of a correlation length for the charge distribution inside the electrode, which can be determined by analyzing

$$\chi_L = \frac{\langle \delta Q^2 \rangle_L}{\langle \delta q^2 \rangle} \frac{\sigma^2}{L^2} - 1, \tag{10}$$

where $\langle \cdot \rangle_L$ is an average over a piece of the electrode $L \times L$ in area, the equivalent electrode atom diameter $\sigma = \sqrt{A/M}$ with A the electrode area and M the corresponding number of atoms. For large enough observation area, the distribution is Gaussian with a variance proportional to the area, as expected from the extensivity of the capacitance. The correlation lengths amount to 2–3 water molecules on Pt, consistent with the surface hydrogen bond network (see Fig. 1) [17,32], and ≈ 6 carbon atoms, consistent with the size of the ions.

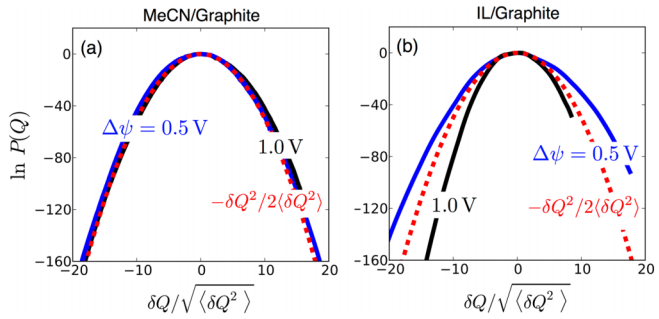

FIG. 4 (color online). Distribution of the total charge for the graphite capacitors, with the MeCN-based electrolyte (a) and pure ionic liquid (b). The results for two applied potentials are compared with Gaussian distributions with the same variance. Note that the variance is the same for both potentials in (a) but is larger at 1 V than at 0.5 V in (b).

The distribution of the total charge is not always Gaussian. Figure 4 compares the distributions at $\Delta\Psi = 0.5$ and 1 V for graphite capacitors with the MeCN-based electrolyte and the pure ionic liquid. While in the former case the distribution is Gaussian with the same variance for both voltages, for the pure ionic liquid this variance increases by a factor of about 2.3 between 0.5 and 1 V. These large fluctuations are reflective of correlations between ions that are not present at low concentration. While the nature of these correlations is beyond the scope of this work, we note that correlations exist that span the electrode sizes we consider here and cause the fluctuations of the total charge on the electrode to be more or less probable than if it was determined from the sum of many uncorrelated charge centers. These aspects of the pure ionic liquid will be considered in detail elsewhere [33].

This sheds new light on the role of correlations on the differential capacitance [34–37]: It measures the susceptibility for the interfacial layer of fluid (at a given potential) to develop charge in response to an increase in the applied potential. It will therefore be low if the fluid is in a particularly stable configuration and resistant to reorganization and large if the fluid has the capability to make a substantial redistribution of charge over the interfacial region.

Combining simulation in the constant-potential ensemble with histogram reweighting techniques has allowed us to investigate correlations in the adsorbed fluid and their influence on the electronic properties of the interface. It further provides a unique way to determine the differential capacitance, more accurately than previously, and from a simulation at a *single* value of $\Delta\Psi$. These methods are based on general principles of statistical mechanics and, as we have shown, are widely applicable [26]. This might prove useful for the study of complex systems such as nanoporous carbon electrodes where the charging mechanism differs from the planar graphite case investigated here [21]. Generalization of this approach to

dynamic properties [38] may lead to new insight on frequency-dependent capacitance measurements and voltage dependence of lubricating properties of IL films on metals [39].

B. R. and D. C. acknowledge financial support from the France-Berkeley Fund under Grant No. 2012-0007. C. M., M. S., and B. R. acknowledge financial support from the French Agence Nationale de la Recherche (ANR) under Grant No. ANR-2010-BLAN-0933-02. We are grateful for the computing resources on JADE (CINES, French National HPC) obtained through the Project No. x2012096728. D. T. L. was supported by the Helios Solar Energy Research Center, which is supported by the Director, Office of Science, Office of Basic Energy Sciences of the U.S. Department of Energy under Award No. DE-AC02-05CH11231.

*benjamin.rotenberg@upmc.fr

[1] P. Simon and Y. Gogotsi, Nat. Mater. **7**, 845 (2008).
[2] D. Brogioli, Phys. Rev. Lett. **103**, 058501 (2009).
[3] D. Brogioli, R. Zhao, and P. M. Biesheuvel, Energy Environ. Sci. **4**, 772 (2011).
[4] N. Boon and R. van Roij, Mol. Phys. **109**, 1229 (2011).
[5] U. Bertocci and F. Huet, Corros. Sci. **51**, 131 (1995).
[6] R. A. Cottis, Corros. Sci. **57**, 265 (2001).
[7] M. A. G. Zevenbergen, P. S. Singh, E. D. Goluch, B. L. Wolfrum, and S. G. Lemay, Nano Lett. **11**, 2881 (2011).
[8] K. Mathwig, D. Mampallil, S. Kang, and S. G. Lemay, Phys. Rev. Lett. **109**, 118302 (2012).
[9] R. Parsons, Chem. Rev. **90**, 813 (1990).
[10] A. A. Kornyshev, J. Phys. Chem. B **111**, 5545 (2007).
[11] Y. Lauw, M. D. Horne, T. Rodopoulos, and F. A. M. Leermakers, Phys. Rev. Lett. **103**, 117801 (2009).
[12] M. Z. Bazant, B. D. Storey, and A. A. Kornyshev, Phys. Rev. Lett. **106**, 046102 (2011).
[13] B. Skinner, T. Chen, M. S. Loth, and B. I. Shklovskii, Phys. Rev. E **83**, 056102 (2011).
[14] C. Gabrielli, F. Huet, and M. Keddam, J. Chem. Phys. **99**, 7232 (1993).
[15] C. Gabrielli, F. Huet, and M. Keddam, J. Chem. Phys. **99**, 7240 (1993).
[16] S. K. Reed, O. J. Lanning, and P. A. Madden, J. Chem. Phys. **126**, 084704 (2007).
[17] A. P. Willard, S. K. Reed, P. A. Madden, and D. Chandler, Faraday Discuss. **141**, 423 (2009).
[18] J. Vatamanu, O. Borodin, and G. D. Smith, J. Am. Chem. Soc. **132**, 14 825 (2010).
[19] S. Tazi, M. Salanne, C. Simon, P. Turq, M. Pounds, and P. A. Madden, J. Phys. Chem. B **114**, 8453 (2010).
[20] C. Merlet, M. Salanne, B. Rotenberg, and P. A. Madden, J. Phys. Chem. C **115**, 16 613 (2011).
[21] C. Merlet, B. Rotenberg, P. A. Madden, P.-L. Taberna, P. Simon, Y. Gogotsi, and M. Salanne, Nat. Mater. **11**, 306 (2012).
[22] C. Merlet, C. Péan, B. Rotenberg, P. Madden, P. Simon, and M. Salanne, J. Phys. Chem. Lett. **4**, 264 (2013).
[23] S. Kondrat and A. Kornyshev, J. Phys. Condens. Matter **23**, 022201 (2011).
[24] J. Siepmann and M. Sprik, J. Chem. Phys. **102**, 511 (1995).
[25] N. Bonnet, T. Morishita, O. Sugino, and M. Otani, Phys. Rev. Lett. **109**, 266101 (2012).
[26] See Supplemental Material at http://link.aps.org/supplemental/10.1103/PhysRevLett.111.106102 for simulation details, derivation of Eqs. (6) and (7) and comparison between the three systems.
[27] J. Johnson, Phys. Rev. **32**, 97 (1928).
[28] H. Nyquist, Phys. Rev. **32**, 110 (1928).
[29] A. M. Ferrenberg and R. H. Swendsen, Phys. Rev. Lett. **63**, 1195 (1989).
[30] S. Kumar, J. M. Rosenberg, D. Bouzida, R. H. Swendsen, and P. A. Kollman, J. Comput. Chem. **13**, 1011 (1992).
[31] B. Roux, Comput. Phys. Commun. **91**, 275 (1995).
[32] D. T. Limmer, A. P. Willard, P. Madden, and D. Chandler, Proc. Natl. Acad. Sci. U.S.A. **110**, 4200 (2013).
[33] C. Merlet, M. Salanne, P. Madden, D. Limmer, D. Chandler, R. van Roij, and B. Rotenberg (to be published).
[34] M. V. Fedorov and A. A. Kornyshev, Electrochim. Acta **53**, 6835 (2008).
[35] S. Lamperski, C. W. Outhwaite, and L. B. Bhuiyan, J. Phys. Chem. B **113**, 8925 (2009).
[36] B. Skinner, M. S. Loth, and B. I. Shklovskii, Phys. Rev. Lett. **104**, 128302 (2010).
[37] M. Drüschler, N. Borisenko, J. Wallauer, C. Winter, B. Huber, F. Endres, and B. Roling, Phys. Chem. Chem. Phys. **14**, 5090 (2012).
[38] C. Nieto-Draghi, J. Perez-Pellitero, and J. B. Avalos, Phys. Rev. Lett. **95**, 040603 (2005).
[39] J. Sweeney, F. Hausen, R. Hayes, G. B. Webber, F. Endres, M. W. Rutland, R. Bennewitz, and R. Atkin, Phys. Rev. Lett. **109**, 155502 (2012).